Key Role of Covalent Bonding in Octahedral Tilting in Perovskites

ARTICLE *in* JOURNAL OF PHYSICAL CHEMISTRY LETTERS · JANUARY 2010

Impact Factor: 7.46 · DOI: 10.1021/jz900399m

THE JOURNAL OF PHYSICAL CHEMISTRY Letters

pubs.acs.org/JPCL

Key Role of Covalent Bonding in Octahedral Tilting in Perovskites

P. Garcia-Fernandez,*,† J.A. Aramburu,† M.T. Barriuso,‡ and M. Moreno†

†Departamento de Ciencias de la Tierra y Física de la Materia Condensada, Universidad de Cantabria, Avda. de los Castros s/n. 39005 Santander, Spain, and ‡Departamento de Física Moderna, Universidad de Cantabria, Avda. de los Castros s/n 39005 Santander, Spain

ABSTRACT Although crystals with perovskite structure have been intensively investigated, there is up to now no clear explanation of why some of them do not remain cubic at low temperature. In particular, the mechanisms of the octahedral tilting in the perovskites have usually been discussed in terms of empirical models based on ion sizes. Here, we show that this important phenomenon is always controlled by changes in covalent bonding through the mixing of occupied and unoccupied orbitals as described by the pseudo-Jahn−Teller effect. These claims are supported by ab initio calculations for the highly ionic perovskite family KMF_3 (M is Ca^{2+} or a 3d transition metal). In particular, it is found that the tilting angle in these compounds depends linearly on the electron population of the π-bonding t_{2g} orbital of the transition metal. This observation is explained using a pseudo-Jahn−Teller model and by studying the calculated electron density of these crystals for different magnetic states.

SECTION Molecular Structure, Quantum Chemistry, General Theory

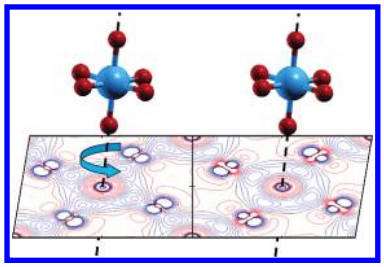

Perovskite materials with the formula ABX_3 (X = F^-, O^{2-}, Cl^-, Br^-, ...) are extremely attractive from both a fundamental and technological point of view because they display a large variety of electrical, magnetic, and structural properties which are, in many cases, sensitive to external perturbations like pressure or temperature. Most of these systems do not correspond with the ideal cubic *Pm3m* perovskite structure at a temperature of $T = 0$ K but undergo structural phase transitions that lower the global symmetry of the crystal. These distortions can be classified according to three kinds of instability, Jahn−Teller (JT), ferroelectric (FE), and antiferrodistortive (AFD). While JT and FE distortions are associated with internal deformations of the BX_6 octahedra, AFD ones are described as coordinated rotations of almost rigid BX_6 octahedra. Understanding the origin of these distortions and the way they interplay is of capital importance to exploit the remarkable properties of these systems. For example, the sign of magnetic coupling constants J depends on the AFD rotation angles,[1] while improper ferroelectricity can be induced due to tilting of the octahedra.[2] The first two types of distortions have been explained in the literature using full quantum mechanical models based on the effect of partially filled degenerate orbitals (JT effect) and the hybridization of empty d or s orbitals localized on B or A cations with occupied p orbitals localized on the X anions (FE distortions),[3] as was first described by Bersuker using a pseudo-Jahn−Teller model (see ref 4). On the other hand, AFD distortions are described by most authors using empirical rules based on steric considerations (size effects) like the Goldschmidt tolerance factor,[5] τ, or bond valence theory.[6] Despite the fact that the Goldschmidt tolerance factor is universally employed as an indicator for the tilting of BX_6 octahedra, it nevertheless presents many shortcomings. For example, τ values[5] do not allow one to clearly specify between cubic and noncubic systems as AFD distortions appear even when $\tau > 1$. Moreover, the τ parameter is able to predict neither the Glazer tilt group[7] in which a given system will stabilize nor the actual value of the rotation angle. Even though these facts are often addressed by the bond valence model, this approach has, however, serious drawbacks because it is a highly parametrized method[6] and thus certainly unsuitable to search for the microscopic origin of the distortions.

Even though the existence of a small covalency plays a key role in understanding many properties in ionic perovskites like ferroelectricity[3] or magnetic superexchange interactions,[8] its effect on the AFD distortions has been rarely considered. Furthermore, works that take into account the existence of covalency often conclude that octahedral tilting is mainly due to steric effects.[5] This Letter is aimed at demonstrating that the tilting of MX_6 octahedra in insulating perovskites is always controlled by changes of covalent bonding through the mixing of occupied and unoccupied orbitals driven by the distortion. To prove the existence of this pseudo-Jahn−Teller (PJT) mechanism,[4] first-principles simulations have been carried out for a large family of fluoroperovskites

Received Date: December 14, 2009
Accepted Date: January 14, 2010

DOI: 10.1021/jz900399m | *J. Phys. Chem. Lett.* **2010**, *1*, 647–651

KMF_3 (M is a divalent metal of the third period, from Ca to Zn) where covalent effects are particularly small and thus often neglected when considering structural distortions. In this family, we find compounds with different structural behavior; while crystals like $KNiF_3$ or $KZnF_3$ are cubic at all temperatures, others, such as $KCaF_3$ or $KMnF_3$, display tilting below a critical temperature.[5] It is worth noting that in this series of compounds, the occupation of σ and π 3d orbitals varies continuously. In this work, we pay particular attention to explore its influence on the existence of tilting. For simplicity, we only consider here one-tilt rotations of $a^0a^0c^-$ or $a^0a^0c^+$ type, leading, respectively, to the space groups *I*4/*mcm* and *P*4/*mbm*. In fact, the former space group is found experimentally[9] at low temperature for some perovskites containing a transition-metal ion in the B position, like $SrTiO_3$ or $KMnF_3$. Also, consideration of only these two space groups allows us to neglect octahedra distortions of JT or FE type.

Density functional theory calculations have been carried out using simulation cells where the basic KMF_3 formula is repeated, respectively, four and two times for *I*4/*mcm* and *P*4/*mbm* space groups. As the insulating antiferromagnetic ground state showed by some of the compounds studied in this work, such as $KNiF_3$ or $KMnF_3$, is incorrectly described by means of local and semilocal functionals of LDA or GGA type, it is necessary to use hybrid functionals to correctly simulate them. We have carried out our calculations employing the hybrid B3LYP functional as implemented in the CRYSTAL06 package.[10] The Bloch wave functions have been represented using localized Gaussian basis sets of approximate double-ζ with polarization quality that have previously been tested to provide a good description of the structural and magnetic properties of the lattices under study.[11] The integration in reciprocal space was carried out by sampling the Brillouin zone with the 8 × 8 × 8 Pack−Monkhorst net, which is enough to provide a full energy convergence. Moreover, strict criteria for the energy (9) and for the evaluation of the Coulomb and exchange series (9,9,9,18) were used. Calculations carried out for antiferromagnetic states require doubling of the unit cell compared to that calculated for the ferromagnetic state to allow for transition-metal ions with spin up and down. In order to reduce the computational cost, we have checked for some selected systems ($KMnF_3$ and $KFeF_3$) that the final geometry for both magnetic states is indistinguishable and carried out the rest of the optimizations for the ferromagnetic state. The tilting angles obtained for *I*4/*mcm* and *P*4/*mbm* space groups are quite similar for all of the studied systems, being slightly larger for the former and accompanied by a stronger stabilization. Thus, we will restrict the discussion to $a^0a^0c^-$-type distortions only. Our calculations provide structural results comparable to those of other authors predicting cubic lattice parameters within 1 % of the experimental results and good agreement in the available tilting angles. For example, we predict that neither $KMgF_3$, $KNiF_3$, nor $KZnF_3$ rotate, in agreement with experiment, while for $KMnF_3$, we predict a rotation angle, θ, of 6.4° that compares well with the experimental result,[9] θ = 5.8°.

Following previous work on the bending of linear ML_2 molecules,[12] like MgF_2 or CaF_2, we have first analyzed the relationship between tilting of MF_6 octahedra in transition-metal fluoroperovskites and the presence of low-lying unoccupied metal π-bonding d orbitals. In MF_6 octahedra, the five levels coming from the d orbitals of M are split into a triplet and a doublet belonging, respectively, to t_{2g} and e_g irreducible representations. The e_g orbital has antibonding σ character and lies at a higher energy than the t_{2g} one that has π character. As a consequence, calculations carried out for the low-spin configuration maximize the number of electrons in the t_{2g} shell, while those for the high-spin configuration minimize them. Figure 1 displays the tilts computed for the KMF_3 family as a function of the number of electrons contained in the t_{2g} shell. Both high-spin and low-spin configurations have been computed for M = Cr^{2+} ($3d^4$ ion in $t_{2g}^3e_g^1$ and $t_{2g}^4e_g^0$ configurations, respectively), Mn^{2+} ($3d^5$ in $t_{2g}^3e_g^2$ and $t_{2g}^5e_g^0$), Fe^{2+} ($3d^6$ in $t_{2g}^4e_g^2$ and $t_{2g}^6e_g^0$), and Co^{2+} ($3d^7$ in $t_{2g}^5e_g^2$ and $t_{2g}^6e_g^1$). Only the ground-state configuration has been considered for the rest of the 3d ions, M = Sc^{2+} ($3d^1$ in $t_{2g}^1e_g^0$), Ti^{2+} ($3d^2$ in $t_{2g}^2e_g^0$), V^{2+} ($3d^1$ in $t_{2g}^3e_g^0$), Ni^{2+} ($3d^8$ in $t_{2g}^6e_g^2$), and Cu^{2+} ($3d^9$ in $t_{2g}^6e_g^3$), and for diamagnetic ions, M = Mg^{2+} ($3s^0$), Ca^{2+} ($4s^03d^0$), and Zn^{2+} ($3d^{10}4s^0$).

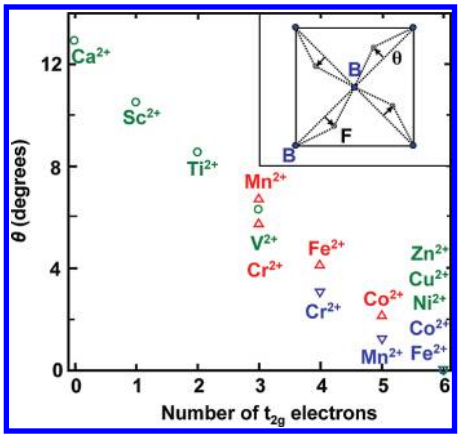

Figure 1. Tilting angle, θ, calculated for the perovskite family KMF_3 (M = Ca−Zn) as a function of the number of electrons contained in the antibonding t_{2g} shell of the transition metal. Results corresponding to compounds calculated in high-spin and low-spin configurations are represented with triangles pointing up (red) and down (blue), respectively. All other systems are represented by green circles, irrespective of their spin. The inset illustrates tilting in a [001] BF_2 plane of the ABF_3 perovskite.

As a salient feature, we can observe in Figure 1 that the calculated distortion angle decreases linearly with the occupation number of the t_{2g} shell along the KMF_3 family. Thus, systems with a full t_{2g} shell, like $KNiF_3$ or $KZnF_3$, do not rotate, while those with empty or nearly empty t_{2g} shells, like $KCaF_3$ or $KScF_3$, rotate the most. Along this line, the rotation angle for the low-spin configuration of $KMnF_3$ (with only one hole in the t_{2g} shell) is found to be practically negligible in comparison to θ = 6.4° calculated for the high-spin configuration which involves three holes in the t_{2g} shell. This situation is somewhat similar to the off-center distortion in ferroelectric perovskites, where it was found that when M is a d^0 ion, the system is more likely to distort due to the PJT coupling between the empty 3d orbitals of the metal and the full 2p orbitals of the ligand.[13] In particular, our calculations indicate that for the empty t_{2g} orbitals of the metal mix with the occupied 2p and 2s orbitals

DOI: 10.1021/jz900399m | *J. Phys. Chem. Lett.* **2010**, *1*, 647–651

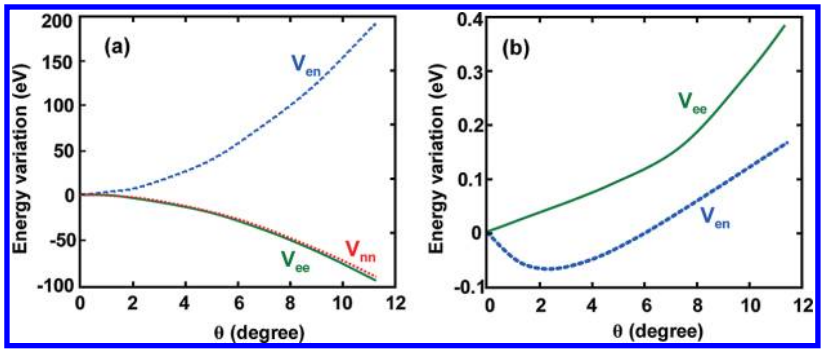

Figure 2. (a) Variation of the V_{ee} (green solid line), V_{en} (blue dashed line), and V_{nn} (red dotted line) contributions to the total energy for high- and low-spin $KMnF_3$ as a function of tilting angle with respect to their value at $\theta = 0$. Note that, due to the large energy scale, high-spin and low-spin curves are completely overlapping. (b) Energy differences between high- and low-spin configurations of $KMnF_3$ corresponding to V_{ee} (green solid line) and V_{en} (blue dashed line) contributions to the total energy.

of fluorine through the rotation due to the lowering of symmetry, thus leading to a change of covalency according to the general behavior of a PJT coupling, this interaction can only give rise to a global energy lowering when the t_{2g} shell is, at least, partially empty. As a consequence, we can understand why high-spin systems rotate more strongly than low-spin ones, thus explaining why $KMnF_3$ rotates but $KNiF_3$ does not. Similar models have allowed us to understand the microscopic origin of various symmetry-breaking distortions in isolated impurities with strongly localized electrons.[14]

In steric models, the driving force for tilting is the reduction of the electron−electron repulsion energy, V_{ee}, between the ion's electron clouds.[6] However, any small symmetry-breaking distortion opens new channels for covalency that involve variations of the electron−nuclei energy, V_{en}. Seeking to clarify the origin of the tilting, we will study first how V_{ee} and V_{en} energies evolve with the rotation angle, while in a second step, we shall explore the small changes on the electronic density induced by the tilting. Since all systems behave similarly, this analysis will be focused on a particular example, $KMnF_3$. In Figure 2a, we plot the variation of V_{ee} and V_{en}, together with the nuclei−nuclei energy, V_{nn}, along the rotation for the high- and low-spin configurations of $KMnF_3$ with respect to their values at $\theta = 0$. It should be emphasized that since we are plotting a difference, the contribution coming from the homogeneous background required to apply the Ewald technique[15] is rigorously canceled, and the values of V_{ee}, V_{en}, and V_{nn} have the same meaning as in molecules. It can be seen that while V_{ee} reduces along the distortion, lowering the total energy, $|V_{en}|$, is also attenuated due to weakening of σ-bonding. It should be noted that the pattern of Figure 2a is found to be fully general in all of the studied systems and appears also in $KMgF_3$ or $KNiF_3$, which do not undergo any rotation. This fact stresses that the existence of tilting is a very subtle phenomenon which requires exploration at a much smaller energy scale. In order to investigate such a phenomenon, we have plotted in Figure 2b the difference between high- and low-spin configurations corresponding to V_{ee} and V_{en} energies as a function of θ with respect to their value at $\theta = 0$. We can notice that for the V_{ee} energy, this difference is positive but less than 0.1 eV for $\theta < 6°$. However, in that region, such a tiny difference is

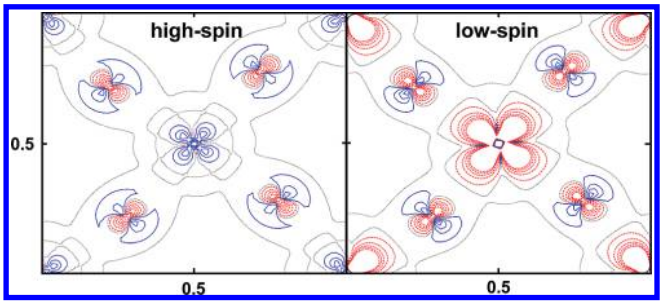

Figure 3. Density deformation plots for $KMnF_3$ on the [001] MnF_2 plane for the high-spin configuration at its equilibrium geometry, $\Delta\rho_{HS}$, and the low-spin configuration at the high-spin equilibrium geometry, $\Delta\rho_{LS}$. Solid blue, dashed red, and dotted black lines represent, respectively, increase, decrease and zero-density contour lines.

compensated by a smaller increase of the V_{en} energy for the high-spin configuration, thus favoring rotation for this configuration. The relative decrease in V_{en} in Figure 2b indicates the creation of new covalencies along the rotation for the high-spin configuration when compared to the low-spin $t_{2g}^5e_g^0$ configuration.

In order to verify this idea, let us now compare the electron density for both high- and low-spin configurations. In Figure 3a, we plot the electron density of the high-spin configuration at its equilibrium geometry with respect to the sum of the density of its isolated ions,[16] which we refer to as $\Delta\rho_{HS}$. An equivalent plot for the low-spin configuration (called $\Delta\rho_{LS}$) at the same geometry is displayed in Figure 3b. These pictures show that there are small but significant differences between the behavior of $\Delta\rho_{HS}$ and $\Delta\rho_{LS}$ around fluorine ions. In particular, it can be noticed that the region around F anions where $\Delta\rho_{HS} > 0$ is more extended than the corresponding domain for $\Delta\rho_{LS}$. Comparison of a and b of Figure 3 shows that zones of charge reinforcement around fluorine anions in high-spin $KMnF_3$ are more delocalized toward the Mn cations. This fact is qualitatively consistent with the existence of a slightly higher covalency for the high-spin configuration than that for the low-spin one and concurs with the conclusions derived from Figure 2b. This outcome is more easily seen in the $\Delta\rho_{HS} - \Delta\rho_{LS}$ plot (in Supporting Information) that

DOI: 10.1021/jz900399m | J. Phys. Chem. Lett. 2010, 1, 647–651

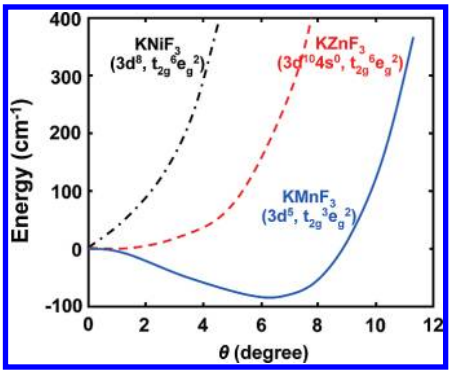

Figure 4. Energy surface cross section along the tilting angle obtained for $KMnF_3$, $KZnF_3$, and $KNiF_3$.

highlights the spatial regions where $\Delta\rho_{HS}$ is larger than $\Delta\rho_{LS}$. The results of Figure 1 can now be related to those of Figures 2 and 3. Indeed, a stronger PJT effect is expected for the high-spin configuration (three holes in the t_{2g} shell) than for the low-spin one with only one hole in the t_{2g} shell. Since electron density changes can only be achieved by mixing full and empty orbitals, the density in the high-spin configuration adapts more easily during the rotation than in the low-spin case, reducing V_{en} and producing larger tilting angles. Our results are fully supported by the recent synchrotron radiation powder diffraction measurements of $KMnF_3$ under high pressure carried out by Aoyagi et al.[17] Using the difference maximum entropy method, they have related the octahedral tilting increase under pressure with a concentration of electrons around the manganese ions due to a stronger Mn-(3d)−F(2p) mixing, a result fully consistent with our PJT model.

Finally, we compare the frequencies of the vibrational modes associated with tilting in the cubic phase of high-spin $KMnF_3$ ($3d^5$ in $t_{2g}^3e_g^2$), $KNiF_3$ ($3d^8$ in $t_{2g}^6e_g^2$), and $KZnF_3$ ($3d^{10}4s^0$ in $t_{2g}^6e_g^4$), whose values are, respectively, 56i, 144, and 30 cm^{-1}. While $KMnF_3$ is unstable and rotates (see Figures 1 and 4), as shown by its imaginary frequency, $KNiF_3$ and $KZnF_3$ are predicted to be cubic (Figure 1), in agreement with experiment and our proposed model since both systems have a full t_{2g} shell. However, these frequency values show that cubic $KNiF_3$ is much more stable with respect to rotation than $KZnF_3$. Inspection of the energy curve along the tilting angle (Figure 4) shows that the curve for $KZnF_3$ is almost flat around the cubic geometry, while $KNiF_3$ quickly gains energy with rotation. Taking into account that the ionic radius of Zn^{2+} is smaller (74 pm) than that of Ni^{2+} (83 pm), the tolerance factor, τ, for $KZnF_3$ is larger than that of $KNiF_3$, indicating that $KNiF_3$ should be more likely to rotate than the former. Thus, we find another contradiction between steric models and ab initio calculations. We have verified that the rotation in $KZnF_3$ is favored because the 4s orbitals in this system are at much lower energies than those in $KNiF_3$. Indeed, inspection of the Mulliken charges for the s shells in Zn^{2+} along the rotation angle show a significant increase in the population not present in $KNiF_3$, supporting this model and explaining why $KZnF_3$ is more likely to tilt even though the radius of Zn^{2+} is smaller than that of Ni^{2+}.

It is important to note that the model presented here is strongly dependent on small details of bonding in the lattice. Thus, substitution of an ion of the lattice may lead to different behavior of the phase transition. For example, replacing K^+ by the more electronegative cation Na^+ leads to tilting when M = Mg^{2+}, Ni^{2+}, or Zn^{2+}, which is not found in the KMF_3 family. However, these rotations do not occur in the $a^0a^0c^-$ Glazer group and instead lead to stabilization in the orthorrombic *Pbnm* group due to tilting along three Cartesian axes. This is an indication that the rotation is not controlled by 3d orbitals since in the latter, the bonding is anisotropic and leads to rotations along a single Cartesian axis.

An interesting test for the conclusions of the present work is to measure the low-temperature structure of KVF_3. Calorimetric measurements have shown that KVF_3 displays magnetic phase transitions at low-temperatures, and it has been argued that they could be associated with structural transitions.[18] According to our calculations (Figure 1), KVF_3 should present a rotation angle similar to that of high-spin $KMnF_3$ at T = 0 K as both have three t_{2g} electrons. Since this rotation is controlled by the t_{2g} orbital, our model predicts that the low-temperature stable structure of KVF_3 belongs to the *I4/mcm* space group.

In conclusion, we have shown that the octahedra tilting in the KMF_3 perovskite family is controlled by the low-lying partially empty t_{2g} shell. This result demonstrates that the proper model to describe the rotation of these systems is the PJT effect, which induces changes in the electronic density following the distortion. The use of this model has many important consequences as, for example, the PJT model predicts that occupied and unoccupied orbitals are, respectively, stabilized and destabilized upon rotation, opening the energy gap between them. Computational studies of systems containing d^1 metals have reported such an increase and associated it with electron localization,[19] providing further support for our work. Along this line, we have verified that a similar electron delocalization from fluorine to the metal is general as it is also present in perovskites formed by closed-shell ions like $KCaF_3$ and $NaMgF_3$, where empty orbitals of the conduction band are responsible for the PJT instability, but not for $KMgF_3$, which, at difference with the previous systems, does not rotate (see Supporting Information). Finally, the behavior of $NaMgF_3$, $NaNiF_3$, and $NaZnF_3$ further suggests that different PJT couplings lead to different final structures, and an assessment of this effect could lead to a much improved understanding of AFD rotations in perovskite crystals. Further research on these issues is currently underway.

SUPPORTING INFORMATION AVAILABLE

Plot of the isodensity contour lines of $\Delta\rho_{HS} - \Delta\rho_{LS}$ for $KMnF_3$ for the high-spin equilibrium geometry in a MnF_2 plane and deformation density contours for $KCaF_3$ and $NaMgF_3$ in MF_2 planes (M = Mg^{2+}, Ca^{2+}). This material is available free of charge via the Internet at http://pubs.acs.org.

AUTHOR INFORMATION

Corresponding Author:

*To whom correspondence should be addressed. E-mail: garciapa@unican.es.

DOI: 10.1021/jz900399m | *J. Phys. Chem. Lett.* **2010**, *1*, 647–651

ACKNOWLEDGMENT The support by the Spanish Ministerio de Ciencia y Tecnología under Project FIS2009-07083 is acknowledged.

REFERENCES

(1) Goodenough, J. B. Theory of the Role of Covalence in the Perovskite-type Manganites [La, M(II)]MnO_3. *Phys. Rev.* **1955,** *100*, 564–573.
(2) Bousquet, E.; Dawber, M.; Stucki, N.; Lichtensteiger, C.; Hermet, P.; Stefano, G.; Triscone, J.-M.; Ghosez, P. Improper Ferroelectricity in Perovskite Oxide Artificial Superlattices. *Nature* **2008,** *452*, 732–737.
(3) Cohen, R. E. Origin of Ferroelectricity in Perovskite Oxides. *Nature* **1992,** *358*, 136–138.
(4) Bersuker, I. B. *The Jahn−Teller Effect*; Cambridge University Press: Cambridge, U.K., 2006.
(5) Woodward, P. M. Octahedral Tilting in Perovskites. II. Structure Stabilizing Forces. *Acta Crystallogr.* **1997,** *B53*, 44–65.
(6) Brown, I. D. Chemical and Steric Constraints in Inorganic Solids. *Acta Crystallogr.* **1992,** *B48*, 553–572.
(7) Glazer, A. M. The Classification of Tilted Octahedra in Perovskites. *Acta Crystallogr.* **1972,** *B28*, 3384–3392.
(8) Anderson, P. W. Antiferromagnetism. Theory of Superexchange Interaction. *Phys. Rev.* **1950,** *79*, 350–356.
(9) Minkiewicz, V. J.; Fujii, Y.; Yamada, Y. X-Ray Scattering and the Phase Transition of $KMnF_3$ at 184 K. *J. Phys. Soc. Jpn.* **1970,** *28*, 443–450.
(10) Dovesi, R.; Orlando, R.; Civalleri, B.; Roetti, C.; Saunders, V. R.; Zicovich-Wilson, C. CRYSTAL: A Computational Tool for the Ab Initio Study of the Electronic Properties of Crystals. *Kristallographiya* **2005,** *220*, 571–573.
(11) Dovesi, R.; Fava, F.; Roetti, C.; Saunders, V. R. Structural, Electronic and Magnetic Properties of KMF_3 (M = Mn, Fe, Co, Ni). *Faraday Discuss.* **1997,** *106*, 173–187.
(12) Garcia-Fernandez, P.; Bersuker, I. B.; Boggs, J. E. Why Are Some ML_2 Molecules (M = Ca, Sr, Ba; L = H, F, Cl, Br) Bent while Others are Linear? Implications of the Pseudo Jahn−Teller Effect. *J. Phys. Chem. A* **2007,** *111*, 10409–10415.
(13) Halasyamani, D. S. Asymmetric Cation Coordination in Oxide Materials: Influence of Lone-Pair Cations on the Intra-octahedral Distortion in d^0 Transition Metals. *Chem. Mater.* **2004,** *16*, 3586–3592.
(14) (a) Garcia-Fernandez, P.; Aramburu, J. A.; Barriuso, M. T.; Moreno, M. Local Symmetry Change in BaF_2:Mn^{2+} at 50 K: Microscopic Insight. *J. Chem. Phys.* **2008,** *128*, 124513. (b) Trueba, A.; Garcia-Fernandez, P.; Barriuso, M. T.; Aramburu, J. A. Pseudo Jahn−Teller Instability in the Axial Fe^+ Center in $KTaO_3$. *Phys. Rev. B* **2009,** *80*, 035131.
(15) Tosi, M. P. Cohesion of Ionic Solids in the Born Model. *Solid State Physics: Advances in Research and Applications*; Academic Press: New York, 1964; Vol. 16, pp 1−120.
(16) (a) Bader, R.F.W. *Atoms in Molecules: A Quantum Theory*; Oxford University Press: Oxford, U.K., 1994. (b) Nakatsuji, H. Electron-Cloud Following and Preceding and the Shapes of Molecules. *J. Am. Chem. Soc.* **1974,** *96*, 30–37.
(17) Aoyagi, S.; Toda, S.; Nishibori, E.; Kuroiwa, Y.; Ohishi, Y.; Takata, M.; Sakata, M. Charge Density Distribution of $KMnF_3$ under High Pressure. *Phys. Rev. B* **2008,** *78*, 224102.
(18) Cros, C.; Chevalier, B. Sur les Fluorures KVF_3 et $RbVF_3$: Étude par Calorimétrie Différentielle et Diffraction X à Basse Température. *Rev. Chim. Miner.* **1977,** *14*, 365–369.
(19) Nuss, J.; Andersen, O. K. How Chemistry Controls Electron Localization in $3d^1$ Perovskites: A Wannier-Function Study. *New J. Phys.* **2005,** *7*, 188.

DOI: 10.1021/jz900399m | *J. Phys. Chem. Lett.* **2010,** *1*, 647–651